Electrochemical characterization of bed electrodes using voltammetry of single granules

Jose Rodrigo Quejigo, Luis F.M. Rosa, Falk Harnisch*

Helmholtz-Centre for Environmental Research GmbH - UFZ, Department of Environmental Microbiology, Permoserstraße 15, 04318 Leipzig, Germany.
Corresponding author: (F. Harnisch) E-mail address: falk.harnisch@ufz.de, Tel.: +49 341 235 - 1337

Abstract

In the search for high surface area electrodes and higher volumetric performances for bioelectrochemical systems, the use of bed electrodes has become a vital field of research. In bed electrodes, conductive particles, i.e. granules, are used as bulk material and are polarized for biofilm growth. One intrinsic constraint of bed electrodes is that these cannot be analyzed by dynamic electrochemical techniques like cyclic voltammetry (CV) due to their high internal resistance and poor polarization behavior. Therefore, solutions to elucidate the extracellular electron transfer (EET) fundamentals in bed electrodes are needed. In this study we show, using the example of a *Geobacter*-based bed electrode, that the thermodynamics of the EET of single granules can be revealed. This is achieved by cyclic voltammetry of single granules. A novel 3D-printed clamp working electrode is presented which can be exploited further for electrochemical analysis of biotic and abiotic electrode particles.

Keywords: microbial extracellular electron transfer, electrochemical analysis, cyclic voltammetry, 3D-printing, microbial fuel cell

* Corresponding author: falk.harnisch@ufz.de (F. Harnisch).

1. Introduction

Microbial electrochemical technologies (MET) are a promising platform for different applications in environmental and industrial biotechnology [1]. MET are based on extracellular electron transfer (EET) processes between electrochemically active microorganisms (EAM) and electrodes [2]. The interaction of EAM and electrode as well as the entire performance of the reactors, termed bioelectrochemical systems (BES), are influenced by the microbiologically accessible electrode surface area. Three-dimensional electrodes, especially granular materials, have been used in recent years to increase this interphase, as they provide a cost-effective approach to creating high electrode surface areas [3]. Granular materials thereby provide a high geometric surface area, but also possess a porous structure that may also increase the real contact between the microorganism and the electrode. Carbon-based materials like coke [4], graphite [5], activated carbon [6] and biochar [7] granules are generally used as bed anodes and cathodes [6, 8]. These materials can be used to assemble beds, which can be either static [9, 10] or moving, i.e. using stirring [11], recirculation [12] or fluidization of the granules [13-15]. The latter approach is energy consuming, but for instance leads to increased current and power production in microbial fuel cells [11].

One inherent limitation of bed electrodes is that these cannot be analyzed using dynamic electrochemical techniques, e.g., cyclic voltammetry (CV) [16]. This can be attributed to their high internal resistance and often poor polarization behavior, which result in insufficient thermodynamic information on microbial bed electrodes. Volumetric current production of EAB developed as part of a single granule BES has already been described [17]. Nonetheless we demonstrate for the first time using the example of a *Geobacter*-based fixed bed anode that cyclic voltammetry of single granules sampled directly from bed electrodes can be performed. This is achieved using a 3D-printed clamp working electrode as part of a setup (Fig. 2A) that allows the study of the previously unknown microbial EET processes occurring in fixed bed electrodes.

2. Materials and methods

All potentials are provided versus Ag/AgCl (sat. KCl) being +0.197 V vs. standard hydrogen electrode (SHE). For all experiments an Ag/AgCl (sat. KCl) electrode (SE11 Sensortechnik Meinsberg, Germany) served as the reference electrode. All chemicals were of at least analytical grade and were supplied by Carl Roth GmbH (Karlsruhe, Germany) and Merck KGaA (Darmstadt, Germany). De-ionized water (Millipore, Darmstadt, Germany) was used in the preparation of all solutions.

2.1. Reactor set-up

During the experiments two different types of reactors were used: a fixed bed BES (Fig. 1A) and a clamp electrochemical cell (Fig. 2A). All experiments were carried out under potentiostatic control using a multi-channel potentiostat/galvanostat (MPG BioLogic Science Instruments, Claix, France).

The fixed bed BES was based on polycarbonate single-chamber cells (250 mL, Nalgene, USA). The counter electrode (CE) consisted of a graphite rod with a geometric surface area of 19.6 cm^2 (CP-Graphite GmbH, Germany). The fixed bed electrode acting as a working electrode (WE) was constituted by 30 cm^3 of unstirred graphite granules (enViro-cell Umwelttechnik GmbH, Oberursel, Germany; diameters from 2 to 3.5 mm, obtained by mechanical sieving). A graphite rod (1 cm^2 geometric surface area, CP-Graphite GmbH, Germany) was vertically embedded into the granule bed acting as a current collector, following the usual general strategy to electrochemically connect bed electrodes [4, 9]. Both CE and WE used 0.5 mm Ø titanium wire as current collector (Goodfellow, UK).

The clamp electrochemical cell (Fig. 2A) was based on four-neck round-bottom flasks, as described previously [18]. The counter electrodes in these cells were made from graphite rods (CP-Handels-GmbH, Germany) with a total projected surface area of 19.6 cm^2. A tailor-made clamp printed from acrylonitrile butadiene styrene (ABS) (Innofil3D, Netherlands) with a 3D printer (Ultimaker 2^+, Ultimaker, Netherlands) acted as a contacting support between a titanium wire and single granules (Fig. 2A). The resistance between wire and granule was below 5 Ω. To avoid diffusion limitation the cell was stirred at 140 rpm using a magnetic stirrer.

All experiments were performed using artificial wastewater according to [19], supplemented with sodium acetate (10 mM) and vitamin and trace metal solutions according to [20]. Prior to the start of the experiment the solution was purged with nitrogen for 30 minutes to ensure anaerobic conditions. The temperature was maintained at 32.5 °C (Incubator Hood TH 15, Edmund Bühler GmbH, Germany).

2.2. Fixed bed BES inoculation and operation

The experiments in fixed bed BES (two independent biological replicates) were inoculated from secondary biofilm anodes, as described elsewhere [18] and operated under batch conditions, replacing the artificial wastewater when current production reached null current. The working electrodes were operated chronoamperometrically (CA) at +0.2 V. The formation of an electrochemically active biofilm on the granules was recognized by a significant increase in current flow and confirmed by fluorescence microscopy analysis. Control measurements were performed using an identical setup but without inserting the current collector into the granule bed.

2.3. Electrochemical analysis of single granules

The experiments in clamp electrochemical cells (five technical replicates) were performed with randomly chosen single granules transferred under oxic atmosphere from the fixed beds to the clamp holders. In total 30 granules (15 granules per fixed bed reactor) were tested. CV of single granules was performed and three cycles were recorded from +0.3 to −0.5 V at a scan rate of 1 $mV \cdot s^{-1}$. The third cycle, showing a steady-state performance, was used for data analysis in accordance with [21]. Control measurements were performed using an identical setup but without graphite particles (titanium wire control) and with abiotic granules (abiotic control). In addition to these analyses, another five extra granules were operated chronoamperometrically at +0.2 V, performing a CV each 6 hours.

2.4 Data analysis and Statistics

The maximum current production (i_{max}), the wet weight of a granule determined after CV measurements in clamp electrochemical cells and the formal potentials (E_f) were each averaged per fixed bed BES, and confidence intervals (CI) at 95% confidence ($p = 0.05$) calculated using the standard deviation and Student-*t* probability distributions for $n = 15$ [22]. To characterize differences between the two fixed bed BESs, analyses were performed using Student's two sample *t*-test of the respective data (OriginPro software (OriginLab, Northampton, USA)). Statistical-tail confidence tests using *t*-values were used to identify outliers from data values ($p > 0.01$) (OriginPro software (OriginLab, Northampton, USA).

3. Results and discussion

3.1. Performance of fixed bed BES

Two fixed bed BESs were operated independently under batch conditions for over two months. They showed stable maximum currents of ca. 25 mA. Fig. 1B shows a typical CV obtained from the fixed bed BES. The undefined shape of the CV is as expected for fixed bed electrodes and does not allow the researcher to infer any information on the underlying EET mechanisms. Fig. 1C shows the CV obtained from the graphite rod serving as current collector in the same system but without connection to the granules (by lifting up the current collector from the fixed bed to the media). Here the voltammogram makes it possible to distinguish two major redox systems at formal potentials of $E_1 = -0.37$ V and $E_2 = -0.17$ V.

In summary, this data shows that properly working, in terms of current production, fixed bed BESs had been established. As expected, no valuable information could be obtained using CV, as the use of porous and granules as fixed bed anodes implies high internal resistance and a heterogeneous potential distribution [23], leading to a poor polarization behavior.

3.2. Cyclic voltammetry analysis of single granules

Single granules of graphite were analyzed using 3D-printed clamp electrodes (Fig. 2A). The transfer of granules from the fixed bed anodes took place during bioelectrocatalysis, i.e. under turn-over conditions. All CVs of in total 30 granules from the two independent fixed bed BESs showed a similar shape (Fig. 2B and 2C). The electrocatalytic waves obtained by CV possessed two oxidation inflection points (represented by two single maximum in the first derivative) and only one reduction inflection point. These two redox systems have been already described for thin *Geobacter sulfurreducens* biofilms [16]. As the arithmetic mean of the two oxidation points coincides with the inflection point of the reduction, Table 1 just shows one formal potential, E_f, per granule. The average values for the granules from the two replicates of fixed bed BES are E_f = -0.31 ± 0.07 V for reactor 1 and E_f = -0.33 ± 0.03 for reactor 2. Redox-peaks for non-turnover CVs were also detected with a similar midpoint potential of - 0.33 V. The average potentials calculated above for the two fixed bed BESs are not statistically different ($p > 0.05$). This statistical similarity can be attributed to the specific electrochemical selection of 0.2 V as anode potential, acetate as sole electron/carbon donor and *Geobacteraceae* dominated biofilms as inoculum. Additionally, the small size of the fixed bed electrodes in comparison to other studies with fixed bed BESs [4, 9] may attenuate the redox gradient's influence [23]. Nevertheless under more complex reactor conditions the anode potential will be a key factor for triggering different EET mechanisms in the same microorganisms [24] as well as the formation of different microbial communities [25, 26]. For instance, *Shewanella oneidensis* exhibits a different exoelectrogenic physiology when the electrode potential changes [27]. Similarly, in *Geobacter sulfurreducens,* dynamic potential-dependent changes between electron transport pathways that are used selectively depending on the anode potential have been demonstrated [24, 28, 29].

Interestingly, the turnover CVs obtained from 29 out of 30 of the granules differ slightly from the sigmoidal shape normally obtained at solid electrodes, e.g. CV of a thin metabolizing *G. sulfureducens* biofilm [16]. As can be observed in Fig. 2C, a peak (at -0.32 V) decreases and finally disappears after 12 hours of granule polarization and bioelectrocatalytic activity, recovering the reported sigmoidal shape of the turnover CVs. We speculate that this peak might be the result either of limiting diffusion in the pores of the granules due to mass transfer limitation [30, 31], and/or most likely due to a temporary microbial metabolic inhibition from the oxygen exposure during the transfer of the granule from the bed electrode to the clamp electrochemical cell. However, both speculations imply a partial inhibition of the metabolism of the bacterial cells in the granules and result in an increasing proportion of redox centers that are electrically but not metabolically connected to the electrode and hence not contributing to the bioelectrocatalytic current flow [30]. Thus this scenario would present a combination of turnover and non-turnover bioelectrochemical responses yielding these CVs. When the granules are polarized longer the microorganisms become metabolically re-activated and also biofilm growth is possible, leading to the disappearance of the peak (Fig. 2C). Further investigations will be performed to clarify this phenomenon.

Table 1 shows maximum current production at +0.2 V during CV of the granules. Differences in i_{max} obtained for each granule are not significantly different when considering the data obtained from all granules withdrawn from the two fixed bed BESs ($p > 0.05$). Microbial current generation on electrodes is determined by the interphase microorganism–electrode and substrate degradation kinetics [3]. In fixed beds the different individual contacts of granule to granule and their spatial location within the bed electrode, and the granule heterogeneity itself create unique conditions, with the redox gradient being most important [27]. In line with this, fresh granules from the bed BES showed a non-homogeneous biofilm covering under fluorescence microscopy (data not shown). The variable weight of the granule does also not differ significantly between the two fixed bed BESs ($p > 0.05$).

4. Conclusions

In this communication it was demonstrated that by applying cyclic voltammetry at single granules, valuable information on the microbial extracellular electron transfer processes of fixed bed electrodes can be gained. Thus this proof of concept opens the possibility of surveying the electrochemical behavior of microbial communities on granulated electrodes in general, which up to now has not been feasible. In addition, the strategy presented here to analyze single conductive particles can be adapted further, e.g. by studying the influence of redox potentials on microbial trophic relations or the interspecies electron transfer processes [32-34]. The presented results not only allow a better understanding of EET fundamentals of fixed bed BESs, but may serve as a valuable tool to shed light on the relation between electrochemical parameters, the selection of microbial communities and ecological functions. Further, the approach highlights the power of tailored voltammetric techniques for studying microbial electrodes [35], as well as inorganic and organic materials [36].

Conflict of interest statement

The authors declare no conflict of interest.

Acknowledgments

We thank Dr. Benjamin Korth for discussions on CV interpretation and Anne Kuchenbuch for assistance during microscopy. F.H. acknowledges support by the BMBF (Research Award “Next generation biotechnological processes — Biotechnology 2020+”) and the Helmholtz-Association (Young Investigators Group). This work was supported by the Helmholtz-Association within the Research Programme Renewable Energies.

5. References

[1] U. Schröder, F. Harnisch, L.T. Angenent, Microbial electrochemistry and technology: terminology and classification, Energy & Environmental Science, 8 (2015) 513-519.
[2] D.R. Lovley, Live wires: direct extracellular electron exchange for bioenergy and the bioremediation of energy-related contamination, Energy & Environmental Science, 4 (2011) 4896-4906.
[3] Y.Y. Yu, D.D. Zhai, R.W. Si, J.Z. Sun, X. Liu, Y.C. Yong, Three-dimensional electrodes for high-performance bioelectrochemical systems, Int J Mol Sci, 18 (2017) 90.
[4] A. Aguirre-Sierra, T. Bacchetti-De Gregoris, A. Berná, J.J. Salas, C. Aragón, A. Esteve-Núñez, Microbial electrochemical systems outperform fixed-bed biofilters in cleaning up urban wastewater, Environ. Sci.: Water Res. Technol., 2 (2016) 984-993.
[5] M. Di Lorenzo, T.P. Curtis, I.M. Head, S.B. Velasquez-Orta, S.B. Velasquez-Orta, K. Scott, A single chamber packed bed microbial fuel cell biosensor for measuring organic content of wastewater, Water Sci Technol, 60 (2009) 2879-2887.
[6] T.S. Song, Z.S. Yan, Z.W. Zhao, H.L. Jiang, Construction and operation of freshwater sediment microbial fuel cell for electricity generation, Bioprocess Biosyst Eng, 34 (2011) 621-627.
[7] T. Huggins, H. Wang, J. Kearns, P. Jenkins, Z.J. Ren, Biochar as a sustainable electrode material for electricity production in microbial fuel cells, Bioresour Technol, 157 (2014) 114-119.
[8] N. Pous, C. Koch, A. Vilà-Rovira, M.D. Balaguer, J. Colprim, J. Mühlenberg, S. Müller, F. Harnisch, S. Puig, Monitoring and engineering reactor microbiomes of denitrifying bioelectrochemical systems, RSC Adv., 5 (2015) 68326-68333.
[9] K. Rabaey, P. Clauwaert, P. Aelterman, W. Verstraete, Tubular microbial fuel cells for efficient electricity generation, Environmental Science & Technology, 39 (2005) 8077-8082.
[10] H.T. Tran, J.H. Ryu, Y.H. Jia, S.J. Oh, J.Y. Choi, D.H. Park, D.H. Ahn, Continuous bioelectricity production and sustainable wastewater treatment in a microbial fuel cell constructed with non-catalyzed granular graphite electrodes and permeable membrane, Water Sci Technol, 61 (2010) 1819-1827.
[11] J. Liu, F. Zhang, W. He, X. Zhang, Y. Feng, B.E. Logan, Intermittent contact of fluidized anode particles containing exoelectrogenic biofilms for continuous power generation in microbial fuel cells, Journal of Power Sources, 261 (2014) 278-284.
[12] A. Deeke, T.H. Sleutels, T.F. Donkers, H.V. Hamelers, C.J. Buisman, A. Ter Heijne, Fluidized capacitive bioanode as a novel reactor concept for the microbial fuel cell, Environ Sci Technol, 49 (2015) 1929-1935.
[13] S. Tejedor-Sanz, J.R. Quejigo, A. Berná, A. Esteve-Núñez, The planktonic relationship between fluid-like electrodes and bacteria: Wiring in motion, ChemSusChem, 10 (2017) 693-700.
[14] S. Tejedor-Sanz, J.M. Ortiz, A. Esteve-Núñez, Merging microbial electrochemical systems with electrocoagulation pretreatment for achieving a complete treatment of brewery wastewater, Chemical Engineering Journal, 330 (2017) 1068-1074.

[15] S. Tejedor-Sanz, P. Fernández-Labrador, S. Hart, C.I. Torres, A. Esteve-Núñez, *Geobacter* dominates the inner layers of a stratified biofilm on a fluidized anode during brewery wastewater treatment, Frontiers in Microbiology, 9 (2018) 378.
[16] K. Fricke, F. Harnisch, U. Schröder, On the use of cyclic voltammetry for the study of anodic electron transfer in microbial fuel cells, Energy & Environmental Science, 1 (2008) 144-147.
[17] C. Borsje, D. Liu, T.H.J.A. Sleutels, C.J.N. Buisman, A. ter Heijne, Performance of single carbon granules as perspective for larger scale capacitive bioanodes, Journal of Power Sources, 325 (2016) 690-696.
[18] C. Gimkiewicz, F. Harnisch, Waste water derived electroactive microbial biofilms: growth, maintenance, and basic characterization, J Vis Exp, 82 (2013) e50800.
[19] J.R. Kim, B. Min, B.E. Logan, Evaluation of procedures to acclimate a microbial fuel cell for electricity production, Appl Microbiol Biotechnol, 68 (2005) 23-30.
[20] W.E. Balch, G.E. Fox, L.J. Magrum, C.R. Woese, R.S. Wolfe, Methanogens: reevaluation of a unique biological group, Microbiological Reviews, 43 (1979) 260-296.
[21] F. Harnisch, S. Freguia, A basic tutorial on cyclic voltammetry for the investigation of electroactive microbial biofilms, Chemistry, an Asian Journal, 7 (2012) 466-475.
[22] J.C. Miller, J.N. Miller, Basic statistical methods for analytical chemistry. Part I. Statistics of repeated measurements. A review, Analyst, 113 (1988) 1351-1356.
[23] T. Doherty, J.G. Sunderland, E.P.L. Roberts, D.J. Pickett, An improved model of potential and current distribution within a flow-through porous electrode, Electrochimica Acta, 41 (1996) 519-526.
[24] C.E. Levar, C.L. Hoffman, A.J. Dunshee, B.M. Toner, D.R. Bond, Redox potential as a master variable controlling pathways of metal reduction by *Geobacter sulfurreducens*, The ISME Journal, 11 (2017) 741-752.
[25] P.G. Dennis, B. Virdis, I. Vanwonterghem, A. Hassan, P. Hugenholtz, G.W. Tyson, K. Rabaey, Anode potential influences the structure and function of anodic electrode and electrolyte-associated microbiomes, Scientific Reports, 6 (2016) 39114.
[26] C.I. Torres, R. Krajmalnik-Brown, P. Parameswaran, A.K. Marcus, G. Wanger, Y.A. Gorby, B.E. Rittmann, Selecting anode-respiring bacteria based on anode potential: phylogenetic, electrochemical, and microscopic characterization, Environmental Science & Technology, 43 (2009) 9519-9524.
[27] L. Peng, S.-J. You, J.-Y. Wang, Electrode potential regulates cytochrome accumulation on *Shewanella oneidensis* cell surface and the consequence to bioelectrocatalytic current generation, Biosensors and Bioelectronics, 25 (2010) 2530-2533.
[28] R.A. Yoho, S.C. Popat, C.I. Torres, Dynamic potential-dependent electron transport pathway shifts in anode biofilms of *Geobacter sulfurreducens*, ChemSusChem, 7 (2014) 3413-3419.
[29] C.E. Levar, C.H. Chan, M.G. Mehta-Kolte, D.R. Bond, An inner membrane cytochrome required only for reduction of high redox potential extracellular electron acceptors, MBio, 5 (2014) e02034-14.
[30] B. Korth, L.F.M. Rosa, F. Harnisch, C. Picioreanu, A framework for modeling electroactive microbial biofilms performing direct electron transfer, Bioelectrochemistry, 106 (2015) 194-206.
[31] S.M. Strycharz, A.P. Malanoski, R.M. Snider, H. Yi, D.R. Lovley, L.M. Tender,

Application of cyclic voltammetry to investigate enhanced catalytic current generation by biofilm-modified anodes of *Geobacter sulfurreducens* strain DL1vs. variant strain KN400, Energy Environ. Sci., 4 (2011) 896-913.
[32] Z.M. Summers, H.E. Fogarty, C. Leang, A.E. Franks, N.S. Malvankar, D.R. Lovley, Direct exchange of electrons within aggregates of an evolved syntrophic coculture of anaerobic bacteria, Science, 330 (2010) 1413-1415.
[33] D.R. Lovley, Reach out and touch someone: potential impact of DIET (direct interspecies energy transfer) on anaerobic biogeochemistry, bioremediation, and bioenergy, Reviews in Environmental Science and Bio/Technology, 10 (2011) 101-105.
[34] S. Kato, K. Hashimoto, K. Watanabe, Microbial interspecies electron transfer via electric currents through conductive minerals, Proceedings of the National Academy of Sciences, 109 (2012) 10042-10046.
[35] N. Pous, C. Koch, J. Colprim, S. Puig, F. Harnisch, Extracellular electron transfer of biocathodes: Revealing the potentials for nitrate and nitrite reduction of denitrifying microbiomes dominated by *Thiobacillus* sp., Electrochemistry Communications, 49 (2014) 93-97.
[36] F. Scholz, Schröder, U., Gulaboski, R., Doménech-Carbó, A. , Electrochemistry of Immobilized Particles and Droplets, Elsevier (2015).

Figure and table captions:

Table 1: Formal potential (E_f), Maximum current (i_{max}) and wet weight of the granules analyzed by single granules CV. The maximum current is obtained at +0.2 V, the potential used to poise the fixed bed BES anode, from the 3rd CV scan. Blue data are defined as outliers (with a probability higher than 99%, $p > 0.01$) in reference to statistical-tail confidence tests using *t*-values. All the data ($n = 15$) has been considered for the statistical analysis.

Figure 1: (A) Scheme for fixed bed BES. (B) Turnover CV of a bioelectrocatalytic *Geobacter* based fixed bed anode and (C) turnover CV of the current collector in the same system but without connection to the granules (by lifting up the current collector from the fixed bed to the media). The scan rate for CVs was 1 mV s^{-1} (3rd scans are shown).

Figure 2: (A) Photograph of clamp electrochemical cell. Outset: scheme of the 3D-printed clamp. (B) Cyclic voltammogram of a single graphite granule with a *Geobacter* based biofilm. The voltammogram was recorded after transferring the granule to the clamp electrochemical cell. Controls were performed without granules (red color) and with abiotic granules (blue color). Inset: first derivative of the voltammetric curve. (C) Cyclic voltammogram evolution of a graphite granule with a *Geobacter* based biofilm. The scan rate for CVs was 1 mV s^{-1} (3rd scans are shown).

Table 1

	Clamp cell 1			Clamp cell 2			Clamp cell 3			Clamp cell 4			Clamp cell 5		
	E_f (V)	i_{max} (μA)	Weight (mg)	E_f (V)	i_{max} (μA)	Weight (mg)	E_f (V)	i_{max} (μA)	Weight (mg)	E_f (V)	i_{max} (μA)	Weight (mg)	E_f (V)	i_{max} (μA)	Weight (mg)
Fixed bed BES 1	-0.35	105	27	-0.37	1.50	28	-0.37	72	71	-0.30	1.30	14	-0.35	60	53
	-0.39	13	31	-0.29	66	29	-0.36	70	26	-0.37	46	18	-0.27	355	47
	-0.35	35	41	-0.37	103	38	0.11	69	31	-0.37	31	15	-0.30	35	32
Fixed bed BES 2	-0.35	64	27	-0.36	50	30	-0.37	52	18	-0.30	29	20	-0.34	51	20
	-0.37	23	19	-0.29	6	13	-0.35	75	35	-0.37	25	40	-0.35	35	17
	-0.36	56	27	-0.16	42	23	-0.37	66	26	-0.38	8	25	-0.30	86	41
Confidence interval (95%) fixed bed BES 1				E_f (V) = -0.31±0.07			i_{max} (μA) = 70.5±46.4						Weight (mg) = 0.033±0.008		
Confidence interval (95%) fixed bed BES 2				E_f (V) = -0.33±0.03			i_{max} (μA) = 43.5±12.5						Weight (mg) = 0.025±0.004		

Highlights

- 3D-printed clamps allow electrochemical analysis of single granules.
- Thermodynamics of electron transfer at single granules are revealed by cyclic voltammetry.
- 3D-printed clamps allow a better understanding of fundamentals of bed electrodes.

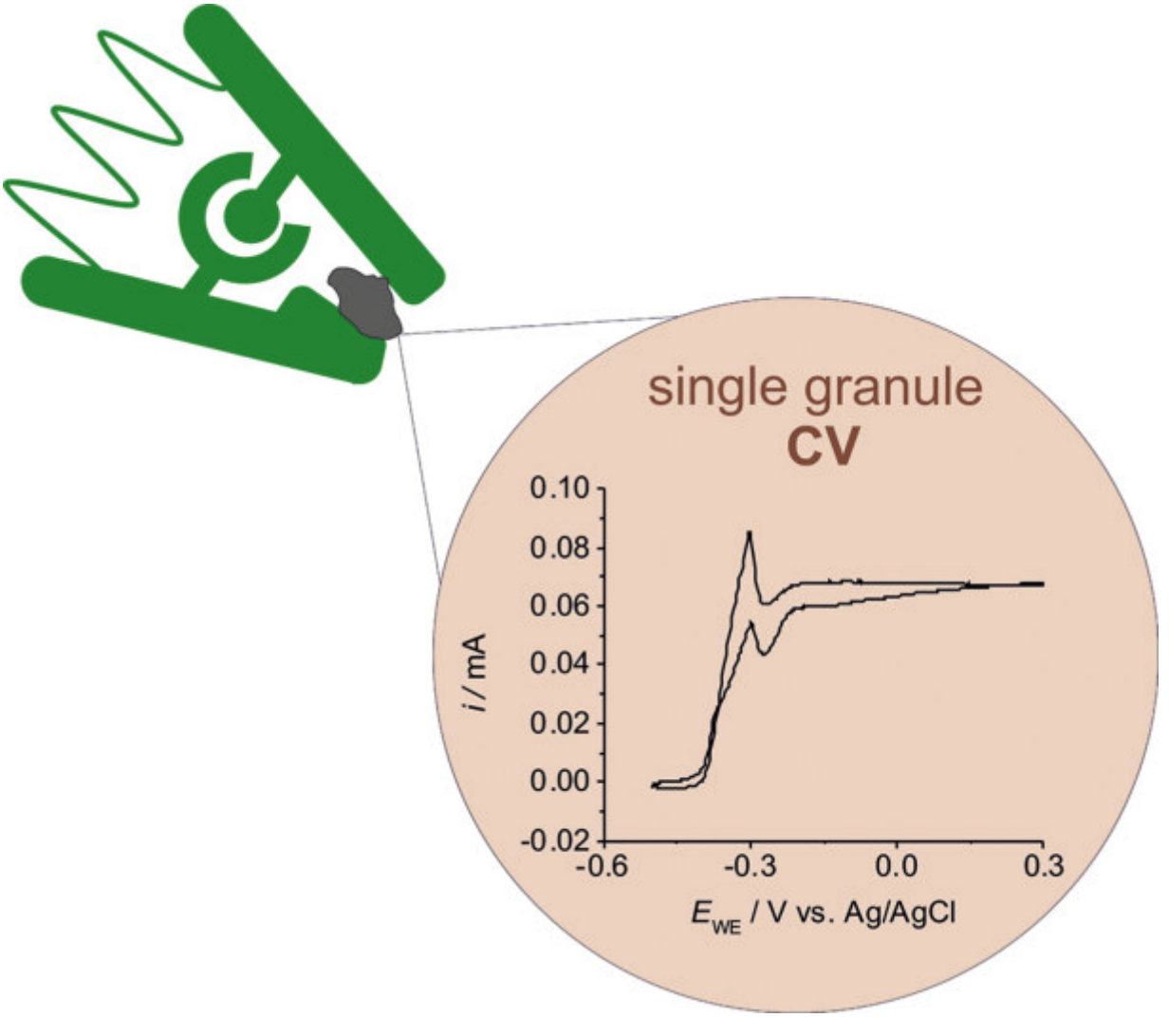

Graphics Abstract

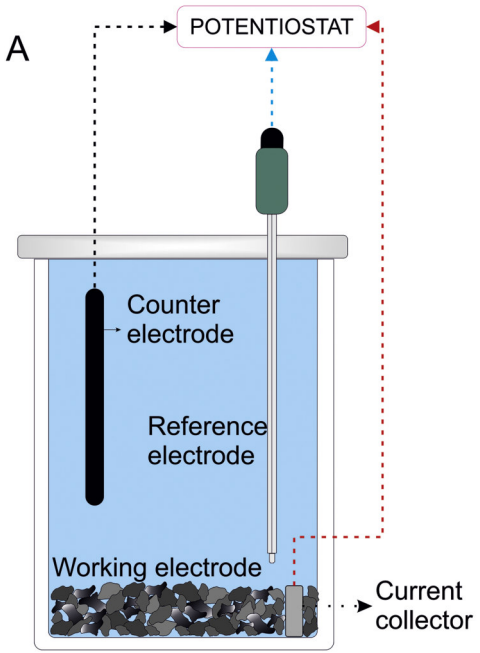
A
POTENTIOSTAT
Counter electrode
Reference electrode
Working electrode
Current collector

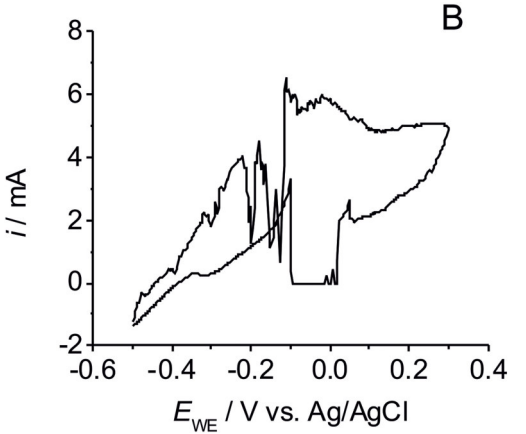
B
i / mA
8
6
4
2
0
-2
-0.6
-0.4
-0.2
0.0
0.2
0.4
E_WE / V vs. Ag/AgCl

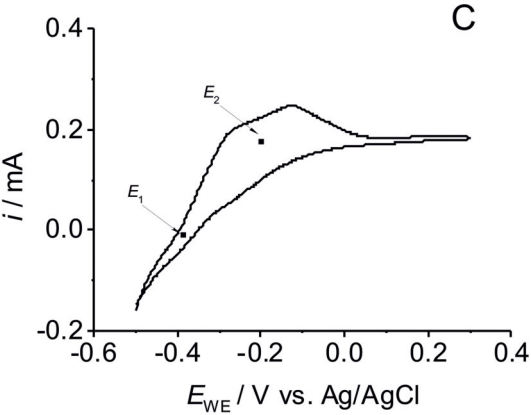
C
i / mA
0.4
0.2
0.0
-0.2
E2
E1
-0.6
-0.4
-0.2
0.0
0.2
0.4
E_WE / V vs. Ag/AgCl

Figure 1

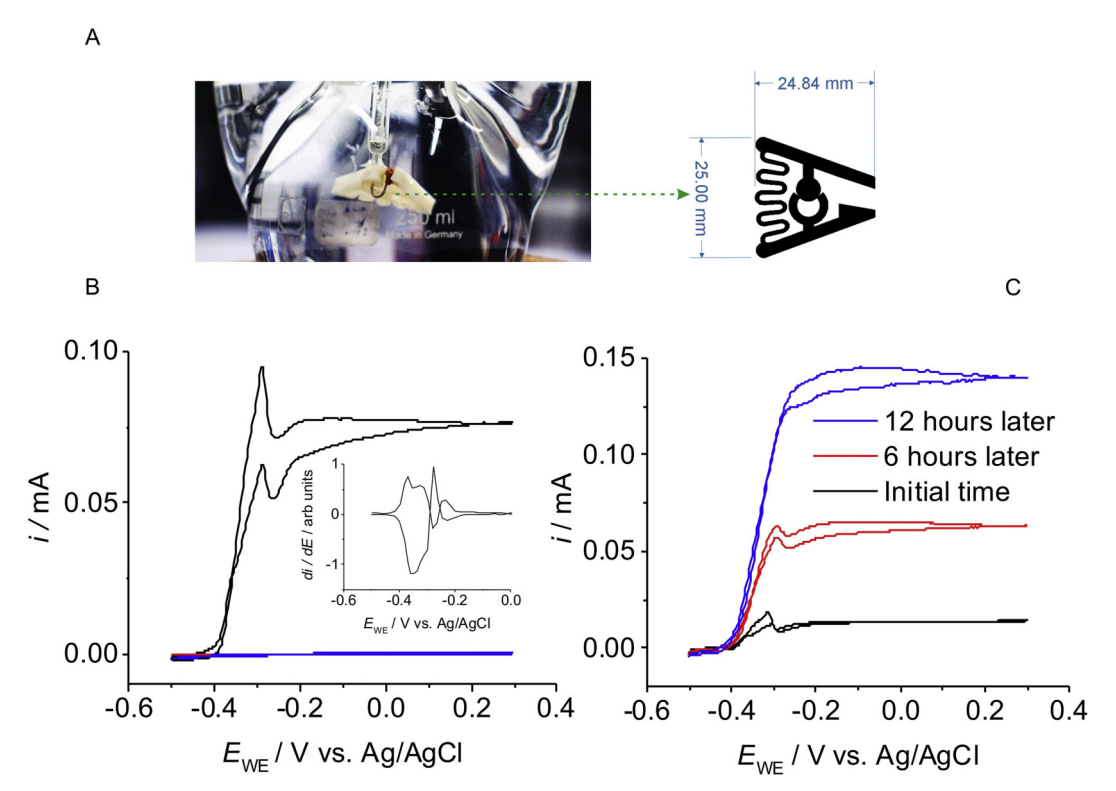
A
250 ml
Made in Germany
24.84 mm
25.00 mm
B
0.10
0.05
0.00
i / mA
-0.6
-0.4
-0.2
0.0
0.2
0.4
E_WE / V vs. Ag/AgCl
1
0
-1
di / dE / arb units
-0.6
-0.4
-0.2
0.0
E_WE / V vs. Ag/AgCl
C
0.15
0.10
0.05
0.00
i / mA
12 hours later
6 hours later
Initial time
-0.6
-0.4
-0.2
0.0
0.2
0.4
E_WE / V vs. Ag/AgCl

Figure 2